

Vinamax: a macrospin simulation tool for magnetic nanoparticles

Jonathan Leliaert · Arne Vansteenkiste · Annelies Coene ·
Luc Dupré · Bartel Van Waeyenberge

Received: date / Accepted: date

Abstract We present Vinamax, a simulation tool for nanoparticles that aims at simulating magnetization dynamics on very large timescales. To this end, each individual nanoparticle is approximated by a macrospin. Vinamax numerically solves the Landau-Lifshitz equation by adopting a dipole approximation method, while temperature effects can be taken into account with two stochastic methods. It describes the influence of demagnetizing and anisotropy fields on magnetic nanoparticles at finite temperatures in a space and time-dependent externally applied field. Vinamax can be used in biomedical research where nanoparticle imaging techniques are under development.

1 Introduction

In recent years, many biomedical applications based on nanotechnology [24] in general and magnetic nanoparticles [28] specifically have emerged. Examples of applications under development are disease detection [21], targeted drug delivery [3] and hyperthermia [20]. All of these depend upon an accurate knowledge of the spatial distribution of the magnetic particles [13, 16] and thus require a nanoparticle imaging technique [6, 25]. Some promising imaging techniques are Magnetic Particle Imaging [18], Magnetorelaxometry [33] and Electron Paramag-

netic Resonance [14]. While each method has its distinct advantages, none of them is able to quantitatively reconstruct the spatial particle distribution *in vivo*. Inadequate knowledge of the spatial distribution of the nanoparticles results in suboptimal applications and even a decrease in patient safety and comfort [14]. The development of an adequate technique is challenging, in part, due to an insufficient understanding of the collective magnetic behaviour of the particles. However, numerically investigating these particles from first principles (i.e. micromagnetically [10]) can lead to an understanding of this collective behaviour and consequently an improved performance of aforementioned applications. To the best of our knowledge there exists no simulation software that both is accurate on the smallest timescales at which micromagnetic dynamics take place, and still is able to simulate the large timescales involved in experiments. Therefore, we have developed Vinamax [2]: a broad simulation tool in which individual nanoparticles are represented by single macrospins. Vinamax numerically solves the Landau-Lifshitz equation [22] and considers demagnetizing and anisotropy fields. It also takes into account externally applied fields that can be space and time-dependent. To be able to simulate large ensembles of nanoparticles the demagnetizing interaction is solved efficiently using a dipole approximation method [30]. This contrasts approaches in which the demagnetizing interaction is not taken into account [5] or cut off after a short distance, e.g. when considering aggregates of nanoparticles [4]. Additionally, thermal effects [11, 17] can be taken into account by two different approaches: first, a stochastic field term can be added to the effective field or second, magnetic nanoparticles are switched at stochastic time intervals, equivalent to the first approach.

J. Leliaert · A. Vansteenkiste · B. Van Waeyenberge
Department of Solid State Sciences, Ghent University, Krijgslaan 281/S1, 9000 Ghent, Belgium
E-mail: jonathan.leliaert@ugent.be

J. Leliaert · A. Coene · L. Dupré
Department of Electrical Energy, Systems and Automation,
Ghent University, Sint-Pietersnieuwstraat 41, 9000 Ghent,
Belgium

The paper is organized as follows. In Section 2 the Landau-Lifshitz equation with the additional stochastic term is described in detail together with the algorithm used to calculate the demagnetizing interaction. Section 3 demonstrates the validity of the software by comparing simulation results to the well-established micromagnetic software MUMAX3[32]. In Section 3.5 the equivalency of both approaches to include thermal effects is demonstrated and a challenging simulation is considered in which one million particles are simulated for one second, as is necessary to simulate a magnetorelaxometry experiment. Finally, some concluding remarks about Vinamax are given in Section 4.

2 Methods

2.1 Micromagnetic theory

In the micromagnetic framework the magnetization is described as a continuum vector field $\mathbf{M}(\mathbf{r}, t)$. In the following the space- and time dependence of the magnetization vector field is no longer explicitly shown in the equations. The nanoparticles under consideration are assumed to be uniformly magnetized[27] (i.e. their size is sufficiently small to be single domain particles). Because all spins within each particle lie parallel to each other, Vinamax can further simplify the continuum approximation by describing every nanoparticle as one single macrospin. This implies that the exchange interactions do not have to be evaluated. The magnetic dynamics of each nanoparticle are described by the Landau-Lifshitz equation (1):

$$\tau = \frac{d\mathbf{m}}{dt} = -\frac{\gamma_0}{1 + \alpha^2} (\mathbf{m} \times \mathbf{B}_{\text{eff}} + \alpha \mathbf{m} \times \mathbf{m} \times \mathbf{B}_{\text{eff}}) \quad (1)$$

In this equation, the torque τ , due to the effective field \mathbf{B}_{eff} felt by each nanoparticle, equals the time derivative of \mathbf{m} , where \mathbf{m} denotes the magnetization vector normalized with respect to the saturation magnetization ($\mathbf{M} = \mathbf{m}M_{\text{sat}}$). Furthermore, γ_0 denotes the gyromagnetic ratio 1.7595×10^{11} rad/Ts and α is the dimensionless Gilbert damping constant. Eq. (1) is solved numerically by timestepping it with timestep Δt , which is described in further detail in section 2.2.

The field \mathbf{B}_{eff} is the sum of the different effective field terms that influence the magnetization:

$$\mathbf{B}_{\text{eff}} = \mathbf{B}_{\text{ext}} + \mathbf{B}_{\text{anis}} + \mathbf{B}_{\text{demag}} + \mathbf{B}_{\text{therm}} \quad (2)$$

The different terms in equation (2) are described in more detail below.

2.1.1 External field

\mathbf{B}_{ext} is an externally applied field that can be both space and time-dependent.

2.1.2 Anisotropy field

In Vinamax the nanoparticles are assumed to have uniaxial anisotropy which is the case for the iron-oxide nanoparticles used in biomedical applications[29]. The field affecting a particle due to this anisotropy is given by equation (3):

$$\mathbf{B}_{\text{anis}} = \frac{2K_{u1}}{M_{\text{sat}}} (\mathbf{m} \cdot \mathbf{u}) \mathbf{u} \quad (3)$$

The anisotropy constant K_{u1} and the anisotropy axis \mathbf{u} can be chosen freely. \mathbf{u} can be set to a predefined direction or to uniformly distributed random directions for all nanoparticles. To this end, two random numbers ϕ and θ are generated with the following distribution:

$$\phi = 2\pi\rho_1 \quad (4)$$

$$\theta = 2 \arcsin(\sqrt{\rho_2}) \quad (5)$$

where $\rho_{1,2}$ denote two uncorrelated, uniformly distributed random numbers in the interval $[0.0, 1.0)$. These spherical coordinates are then mapped to their cartesian counterparts using the well-known relations below:

$$x = \sin(\theta) \cos(\phi) \quad (6)$$

$$y = \sin(\theta) \sin(\phi) \quad (7)$$

$$z = \cos(\theta) \quad (8)$$

2.1.3 Demagnetizing field

The demagnetizing field (or the magnetostatic interaction) results from the dipole-dipole interaction of the different particles. Its contribution to the effective field is given by equation (9), where i loops over all particles, $\mu_0 = 4\pi \times 10^{-7}$ T/Am, \mathbf{r}_i denotes the distance from each particle to the point at which the demagnetizing field is evaluated, and V_i is the volume of each particle.

$$\mathbf{B}_{\text{demag}} = \mu_0 \sum_i V_i M_{\text{sat},i} \left[3 \frac{(\mathbf{m}_i \cdot \mathbf{r}_i) \mathbf{r}_i}{r_i^5} - \frac{\mathbf{m}_i}{r_i^3} \right] \quad (9)$$

2.1.4 Dipole approximation method

To speed up the evaluation of the demagnetizing field, we have implemented a dipole approximation method. This method is based on a multipole approximation described in Ref. [30]. We will briefly describe our adapted implementation, but for a detailed explanation we refer

to Ref. [30].

In Vinamax, the user has to define a *world*, which is a cube that encloses all the particles in the simulation. This cube is then subdivided into 8 subnodes, which are further subdivided until every node contains at most one particle. Within this tree, we then calculate the *center of magnetization* once for every node. The center of magnetization (CM) is the center of mass of the particles in the node weighted with the magnetic moment of each particle. This is shown in eq. (10), where \sum_i denotes a sum over all particles in the node, and \mathbf{r}_i is the position of particle i .

$$\mathbf{R}_{\text{CM}} = \frac{1}{\sum_i V_i M_{\text{sat},i}} \sum_i \mathbf{r}_i V_i M_{\text{sat},i} \quad (10)$$

In the evaluation of the total demagnetizing field we take into account the contribution per node of the field \mathbf{B}_d as if all the particles in a node were compressed into one dipole in the CM of that node, using eq. (11), where \mathbf{r} denotes the distance between the CM of the node and the point at which the field is evaluated. Before every timestep, the magnetization $\mathbf{M} = \sum_i V_i M_{\text{sat},i} \mathbf{m}_i$ of each node is updated based on the magnetization of every particle within the nodes.

$$\mathbf{B}_d = \mu_0 \frac{3(\mathbf{M} \cdot \mathbf{r})\mathbf{r} - \mathbf{M}}{r^3} \quad (11)$$

For every particle, the demagnetizing field working on it is evaluated with the algorithm described in Fig. 1, copied from Ref. [30] with minor adaptations to our implementation.

This algorithm only requires work of $\mathcal{O}(N \log(N))$, while the direct pairwise evaluation of the demagnetizing field (from now on called *brute force method*) between N particles (eq. (9)) scales as $\mathcal{O}(N^2)$. These statements are validated in section 3.

2.1.5 Stochastic thermal field

The effective field \mathbf{B}_{eff} includes a stochastic term $\mathbf{B}_{\text{therm}}$ to take thermal fluctuations [15] into account. Brown[11] has worked out the detailed properties of this stochastic field for a single domain particle with the use of the fluctuation-dissipation theorem, which led to eq. (12).

Because in Vinamax each particle is approximated by one single macrospin, it is particularly suitable to

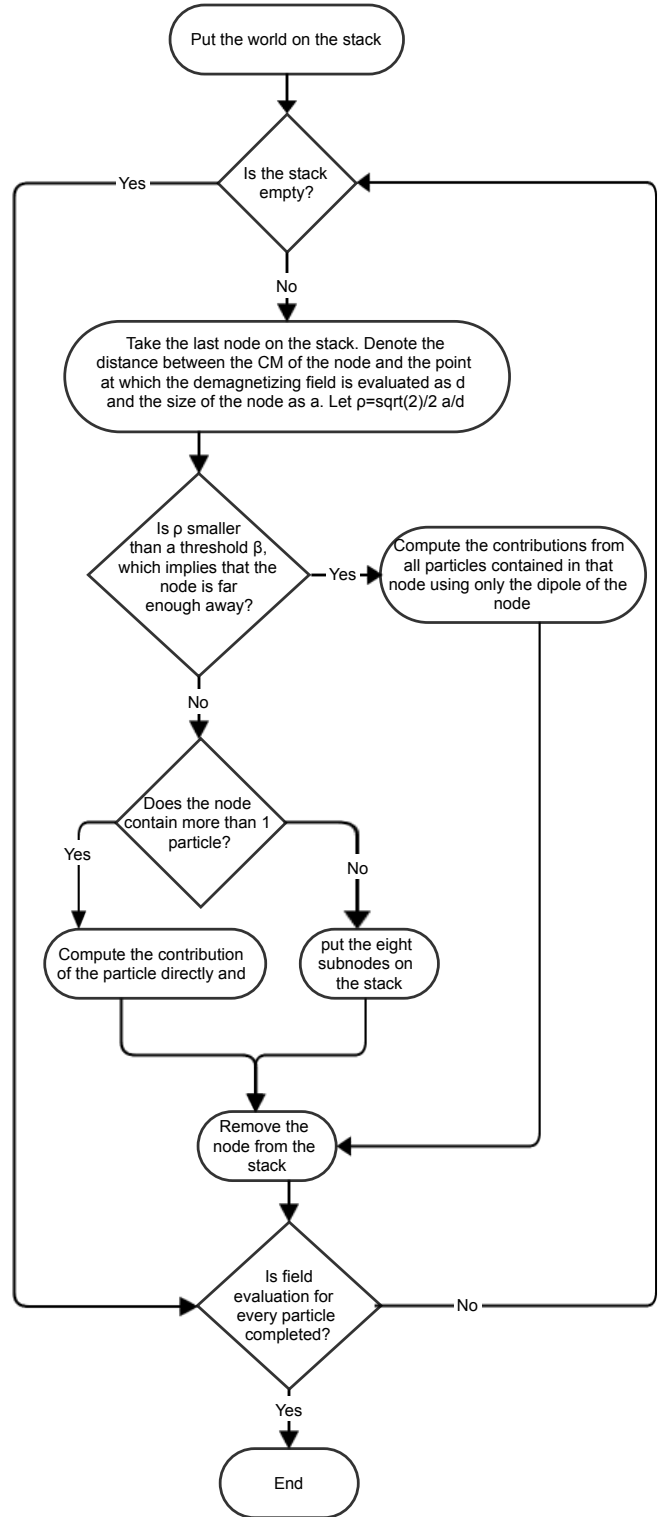


Fig. 1 The algorithm used to evaluate the demagnetizing field, adapted from Ref. [30].

use Brown's theory. So the equation we implemented reads

$$\mathbf{B}_{\text{therm}}(t) = \eta(t) \sqrt{\frac{2k_B T \alpha}{\gamma_0 M_{\text{sat}} V \Delta t}} \quad (12)$$

where $\eta(t)$ denotes a random vector whose components are normal distributed random numbers with mean 0 that are uncorrelated in space and time, Δt is the timestep and k_B is the Boltzmann constant.

2.1.6 Stochastic switching

The approach with the stochastic field of section 2.1.5 has a large computational cost. Therefore, also a faster implementation based on stochastic switching of the nanoparticles is presented. This approach, however has the drawback that it is only valid in a constant field.

For a single domain particle with uniaxial anisotropy eq. (12) leads to switching between two states with minimal energy, separated by an energy barrier of height $\Delta E = K_{u1} V$ with a switching rate f :

$$f = f_0 \exp\left(\frac{-\Delta E}{k_B T}\right) \quad (13)$$

In the high barrier limit ($\Delta E \ll k_B T$) f_0 is equal to [9, 31, 11]

$$f_0 = \frac{\alpha \gamma}{1 + \alpha^2} \sqrt{\frac{H_K^3 M_s V}{2\pi k_B T}} \left(1 - \frac{H}{H_K}\right) \left(1 - \frac{H^2}{H_K^2}\right) \quad (14)$$

with $H_K = 2K_{u1}/M_s$.

The probability that a particle does not switch during a certain time ΔT is given by $\frac{dP_{\text{not}}}{dt} = -f P_{\text{not}}$ [9]. In a constant field this leads to

$$\ln P_{\text{not}} = \int_0^{\Delta T} f dt \Rightarrow P = 1 - \exp(-f \Delta t) \quad (15)$$

The next switching time for a particle can thus be generated with $t = -\frac{1}{f} \ln(1 - P)$ by generating a random number P , uniformly distributed between 0 and 1 [23]. When the simulation reaches this time, the magnetization of the particle is switched to its opposite direction and a new switching time is generated.

2.2 Time integration schemes

Vinamax provides the user with a wide range of different methods to numerically integrate eq. (1). [12]

- Euler's method

- Heun's method
- 3th order Runge Kutta method
- 4th order Runge Kutta method
- Dormand-Prince (5th order, adaptive step)
- Fehlberg method (6th order, adaptive step)
- Fehlberg method (7th order, adaptive step)

The adaptive timestep methods incorporate a lower-order scheme, which provides an estimate of the error on the obtained results. Using eq.(16)[19], in which O stands for the order of the solver, it is then possible to estimate an optimal timestep dt_{opt} based on the error tolerance ϵ which can be set by the user.

$$dt_{\text{opt}} = dt_{\text{current}} \left(\frac{\epsilon}{dt_{\text{current}} \tau_{\text{max}}} \right)^{(1/O)} \quad (16)$$

Note that adaptive timesteps can not be used when using the stochastic thermal field, as the size of this field depends on the timestep (eq. (12)), which turns eq. (16) unstable. Because the thermal fields should be uncorrelated in time [11] the timestep should not be set smaller than 1e-13 s.

3 Results

The use of the macrospin approximation in Vinamax has the advantage that exchange interactions do not have to be evaluated. However, this has the drawback that the micromagnetic standard problems[1], which do incorporate exchange interactions, can not be solved by Vinamax. In this section we therefore simulate some simple, yet general, problems and compare their solution with the micromagnetic simulation software MUMAX3[32].

3.1 Problem one: Precession and Damping

In this first problem an isotropic single particle is considered at 0 K. It is initialised with the magnetization along the x-direction and an external field of 10 mT is applied along the z-direction. The magnetization gyrates around this axis with a frequency of 28 GHz/T and slowly damps towards the z-axis, as dictated by the Landau-Lifshitz equation.

In Fig. 2 the results of the simulation are shown. The oscillations in the x- and y-components of the magnetization have a frequency of 0.28 Ghz, which is in agreement with both the theoretically expected value and the result obtained with MUMAX3. The steady increase of the z-component of the magnetization corresponds with the damping towards the z-axis ($\alpha = 0.02$).

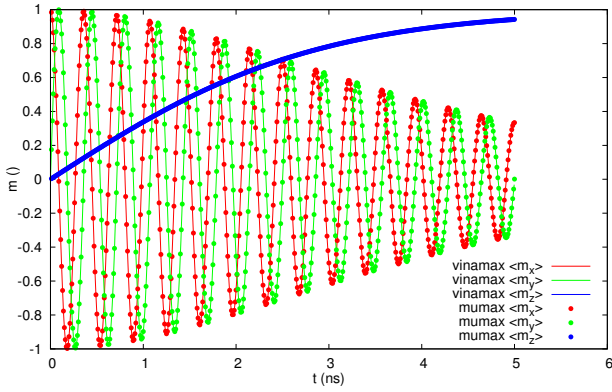


Fig. 2 The average magnetization components as a function of time for simulation problem one. The magnetization precesses around the z-axis with a frequency of 0.28 GHz and slowly damps towards this axis. The different colours denote the different magnetization components. The full lines denote the results obtained with Vinamax, while the dots correspond to the results obtained with MuMax3.

3.2 Problem two: Magnetostatic Interaction

The aim of the second problem is to show that the brute force method to calculate the demagnetizing field is implemented correctly. To this end, at 0 K, two isotropic nanoparticles relax in the presence of an external field of 1 mT along the x-axis. The same simulation is also repeated without calculating the demagnetizing field to see that this problem is suited to validate the implementation; i.e. to see that the demagnetizing field has an influence.

The nanoparticles have a diameter of 32 nm and a saturation magnetization of 860000 A/m. The damping constant α was set to 0.1.

Again, the results are validated by comparing the results from Vinamax with those from MuMax3. In Fig. 3 it can be seen that the demagnetizing field is of significant importance in this problem and that the simulation results correspond with each other.

3.3 Problem three: Dipole Approximation method

This example shows the agreement between the dipole approximation implementation and the brute force implementation. The same problem is also solved without taking this interaction into account so to illustrate that it is of importance in this system.

In this problem 256 isotropic nanoparticles with a diameter of 32 nm and saturation magnetization 860000 A/m are created with a spatially uniform distribution

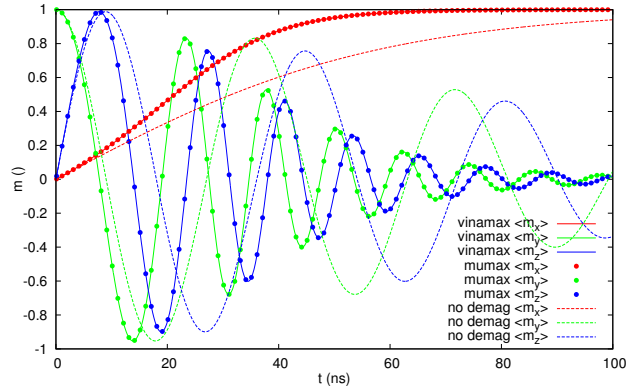


Fig. 3 The average magnetization components (different colours) as a function of time for simulation problem two. The dashed lines show the dynamics for the case in which the demagnetizing field is not included in the simulation. The full lines and big dots show the simulation results (with the demagnetizing field) obtained with Vinamax and MuMax3 respectively. Both results are in correspondence with each other.

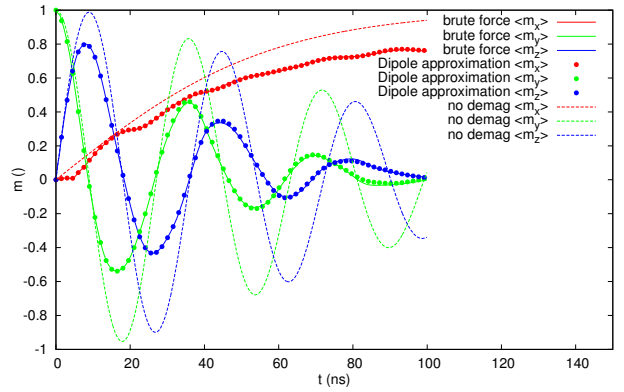


Fig. 4 The average magnetization components (different colours) as a function of time for simulation problem three. The dashed lines illustrate that the demagnetizing field has an influence in this problem. The full lines and the dots correspond with the results obtained using the brute force or dipole approximation method (with $\beta = 0.4$) respectively in Vinamax, and are in correspondence with each other.

in a cube with a side of $2 \mu\text{m}$ with their magnetization along the z-axis. They relax at 0 K in the presence of an external field of 1 mT along the x-axis ($\alpha = 0.1$). In Fig. 4 the results of these simulations are visualised.

We have also investigated the performance of the different methods for evaluating the demagnetizing field in Vinamax. Fig. 5 shows the scaling behaviour of the time it takes to calculate one timestep with the brute force evaluation of the demagnetizing field versus the dipole approximation method. All simulations were performed on an Intel Core i7-3770 CPU @ 3.40GHz. The brute force method scales as $\mathcal{O}(N^2)$. The dipole approximation method is slower for smaller numbers of

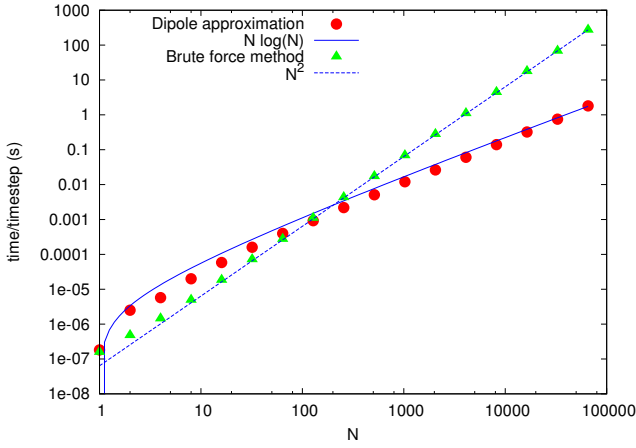


Fig. 5 The time necessary to calculate one timestep, with Heun’s solver, as function of N , the number of particles in the system. The green triangles correspond with the brute force evaluation of the dipole-dipole interactions, while the red dots correspond with the dipole approximation method. To visualize the scaling behaviour of both algorithms, a fit to a function $\sim N^2$ (blue dots) and $\sim N \log(N)$ (blue line) is shown.

particles, but scales as $\mathcal{O}(N \log(N))$. From 512 particles on, the dipole approximation method is faster than the brute force calculation and for large numbers of particles this results in an enormous speedup of the simulation. Note that we adapted the volume of the simulation to the number of particles to keep the concentration of the particles constant.

3.4 Problem four: Lognormal diameter distribution

As the distribution of nanoparticle diameters D often follows a lognormal distribution[33,8], the diameter of the particles in Vinamax can also be drawn from such a distribution, as shown in Fig. 6. Eq. (17) shows the probability density function $P(D)$ for a lognormal distribution with μ and σ the mean and standard deviation of the logarithm of the diameter.

$$P(D) = \frac{1}{\sqrt{2\pi}\sigma D} \exp\left(-\frac{\ln^2(D/\mu)}{2\sigma^2}\right) \quad (17)$$

Problem four shows how an ensemble of 20000 particles at 0 K, which are initially magnetized with their magnetization along the z-axis, relaxes towards a randomly chosen (per particle) anisotropy direction. The magnetization of each particle relaxes towards its anisotropy axis in the direction above the horizontal plane. After a short relaxation time, the average magnetization is thus expected to be $\int_0^{\pi/2} \sin(x) \cos(x) dx = 0.5$. Fig. 6 shows that this is indeed the case.

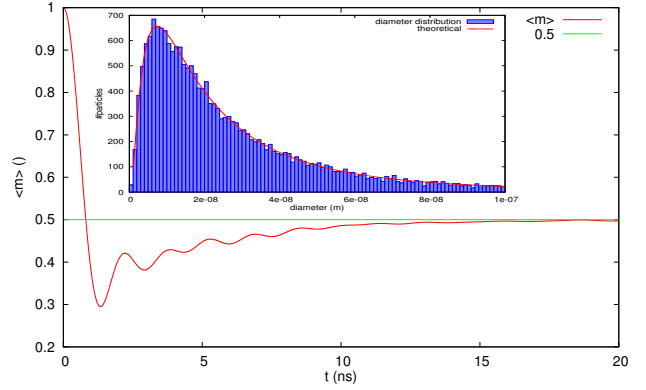


Fig. 6 The average magnetization $\sqrt{(m_x^2 + m_y^2 + m_z^2)}$ versus time. The magnetization relaxes towards 0.5, as predicted analytically. Inset: the particle size distribution for problem four. 20000 particles were created with their diameter drawn from a lognormal distribution with $\mu = 20$ nm and $\sigma = 1$ nm. The theoretical distribution function for these values (eq. (17)) is shown in red to show the correspondence.

3.5 Application: Thermal switching time distribution and magnetization relaxation

In the previous section 3.4 the magnetic relaxation of an ensemble of nanoparticles was shown on the nanosecond timescale. The subject of this section is the thermal Néel relaxation at a much larger timescale.

In an ensemble of single domain particles with uniaxial anisotropy, there exist two ground states along the anisotropy axis for every particle. Due to thermal fluctuations, the magnetization of each particle will switch between these two directions at random intervals. The total magnetization of the ensemble will thus slowly relax towards 0. The rate of this relaxation is given by the Néel relaxation time[26] τ_N , eq. (18).

$$\tau_N = \tau_0 \exp\left(\frac{K_u V}{k_B T}\right) \quad (18)$$

In this equation, τ_0 is an extinction time with values between 10^{-8} and 10^{-12} s [33,7], and is related to f_0 (eq. (14)) by $\tau_0 = \frac{1}{2f_0}$.

In this problem we look at the distribution of switching times of uniaxial particles with a diameter of 25 nm. As can be seen in inset Fig. 7, both approaches (a stochastic thermal field (section 2.1.5) and stochastic switching (section 2.1.6)) show good agreement in the distribution of switching times.

The result of a lot of these switches on the magnetization is given by[33]

$$m = \int_V m_0 \exp\left(-\frac{t}{\tau_N(V)}\right) P(V) dV \quad (19)$$

which equals $m = m_0 \exp\left(-\frac{t}{\tau_N}\right)$ for particles of equal size. In Fig. 7 the resulting magnetization of an ensemble

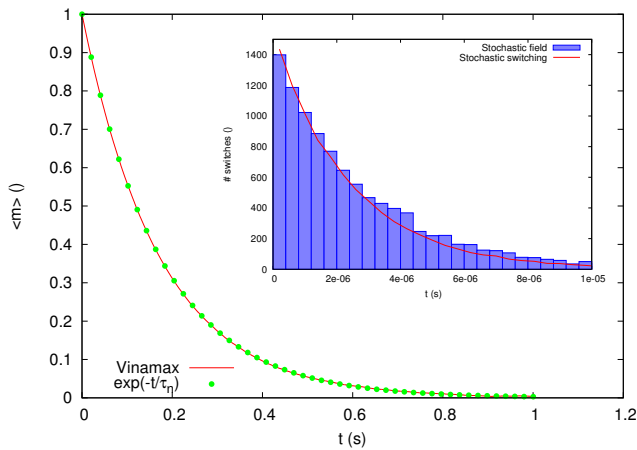


Fig. 7 The magnetization as function of time for an ensemble of one million nanoparticles. Because of this large number, there are no fluctuations visible and the relaxation curve exactly follows the theoretical curve. The simulated nanoparticles have a saturation magnetization of 400000 A/m and uniaxial anisotropy of 10000 J/m³, along the z-axis. They are simulated at a temperature of 300 K. The diameter of the particles is 25 nm and $\alpha = 0.05$. The particles are placed far enough apart to neglect the demagnetizing field. The inset shows the switching time distribution for one particle with a diameter of 18 nm for two approaches to take thermal effects into account. The particle with the stochastic field was simulated until it switched 10000 times (blue bars) and the particle with the stochastic switching (red line) was simulated until 100000 switching events were recorded (rescaled to 10000, to be able to compare both distributions). Both approaches show good agreement on the switching time distribution.

ble of one million particles is shown, together with the analytical result of eq. 19.

4 Discussion

The aim of this paper is to present Vinamax: a numerical software package that performs micromagnetic simulations of magnetic nanoparticles, approximated by macrospins. We have validated Vinamax in various problems against other micromagnetic software (MuMAX3) and analytical results. Each problem (sections 3.1 to 3.4) shows that a different part of Vinamax is implemented correctly and the results correspond well to the expected ones. In section 3.5 Vinamax is then used to solve a challenging problem. Due to the dipole approximation method that scales as $\mathcal{O}(N \log(N))$ with N the number of particles, it is possible to simulate systems with large amounts of particles, and on large timescales. We emphasize that vinamax can be used as a research tool in biomedical applications, where we especially aim at nanoparticle imaging techniques, such as relaxometry where the collective effect of nanoparticles still is not completely understood. In this domain Vinamax

could for example be used to investigate the effect of the dipolar interaction on the relaxation curves.

J.L. Would like to thank M. Dvornik for fruitful discussions. This work is supported by the Flanders Research Foundation (A.V.)

References

1. <http://www.ctcms.nist.gov/mumag/mumag.org.html>
2. Vinamax website: <http://jleliaert.github.io/vinamax/>
3. Alexiou, C., Arnold, W., Klein, R., Parak, F., Hulin, P., Bergemann, C., Erhardt, W., Wagenpfeil, S., L  bbe, A.: Locoregional cancer treatment with magnetic drug targeting. *Cancer research* **60**(23), 6641–6648 (2000)
4. Andreu, J.S., Calero, C., Camacho, J., Faraudo, J.: On-the-fly coarse-graining methodology for the simulation of chain formation of superparamagnetic colloids in strong magnetic fields. *Phys. Rev. E* **85**, 036709 (2012). DOI 10.1103/PhysRevE.85.036709. URL <http://link.aps.org/doi/10.1103/PhysRevE.85.036709>
5. Babinec, P., Kraf  k, A., Babincov  , M., Rosenecker, J.: Dynamics of magnetic particles in cylindrical halbach array: implications for magnetic cell separation and drug targeting. *Medical & biological engineering & computing* **48**(8), 745–753 (2010)
6. Baumgarten, D., Liehr, M., Wiekhorst, F., Steinhoff, U., M  nster, P., Miethe, P., Trahms, L., Hauelsen, J.: Magnetic nanoparticle imaging by means of minimum norm estimates from remanence measurements. *Medical & biological engineering & computing* **46**(12), 1177–1185 (2008)
7. Bessais, L., Ben Jaffel, L., Dormann, J.L.: Relaxation time of fine magnetic particles in uniaxial symmetry. *Phys. Rev. B* **45**, 7805–7815 (1992). DOI 10.1103/PhysRevB.45.7805. URL <http://link.aps.org/doi/10.1103/PhysRevB.45.7805>
8. Branquinho, L.C., Carri  o, M.S., Costa, A.S., Zufelato, N., Sousa, M.H., Miotto, R., Ivkov, R., Bakuzis, A.F.: Effect of magnetic dipolar interactions on nanoparticle heating efficiency: Implications for cancer hyperthermia. *Scientific reports* **3** (2013)
9. Breth, L., Suess, D., Vogler, C., Bergmair, B., Fuger, M., Heer, R., Brueckl, H.: Thermal switching field distribution of a single domain particle for field-dependent attempt frequency. *Journal of Applied Physics* **112**(2), 023903 (2012). DOI <http://dx.doi.org/10.1063/1.4737413>. URL <http://scitation.aip.org/content/aip/journal/jap/112/2/10.1063/1.4737413>
10. Brown, W.F.: *Micromagnetics*. 18. Interscience Publishers New York (1963)
11. Brown, W.F.: Thermal fluctuations of a single-domain particle. *Phys. Rev.* **130**, 1677–1686 (1963). DOI 10.1103/PhysRev.130.1677. URL <http://link.aps.org/doi/10.1103/PhysRev.130.1677>
12. Butcher, J.C.: *Numerical methods for ordinary differential equations*. John Wiley & Sons (2008)
13. Coene, A., Crevecoeur, G., Dupre, L.: Adaptive control of excitation coil arrays for targeted magnetic nanoparticle reconstruction using magnetorelaxometry. *IEEE Trans. Magn.* **48**(11), 2842–2845 (2012). DOI 10.1109/TMAG.2012.2201706. International Magnetics Conference (INTERMAG), Vancouver, CANADA, MAY 07–11, 2012

14. Coene, A., Crevecoeur, G., Dupré, L., Vaes, P.: Quantitative estimation of magnetic nanoparticle distributions in one dimension using low-frequency continuous wave electron paramagnetic resonance. *Journal of Physics D: Applied Physics* **46**(24), 245,002 (2013). URL <http://stacks.iop.org/0022-3727/46/i=24/a=245002>
15. Coffey, W.T., Kalmykov, Y.P.: Thermal fluctuations of magnetic nanoparticles: Fifty years after brown. *Journal of Applied Physics* **112**(12), 121301 (2012). DOI <http://dx.doi.org/10.1063/1.4754272>. URL <http://scitation.aip.org/content/aip/journal/jap/112/12/10.1063/1.4754272>
16. Eichardt, R., Baumgarten, D., Petković, B., Wiekhorst, F., Trahms, L., Haueisen, J.: Adapting source grid parameters to improve the condition of the magnetostatic linear inverse problem of estimating nanoparticle distributions. *Medical & biological engineering & computing* **50**(10), 1081–1089 (2012)
17. Evans, R.F.L., Hinzke, D., Atxitia, U., Nowak, U., Chantrell, R.W., Chubykalo-Fesenko, O.: Stochastic form of the landau-lifshitz-bloch equation. *Phys. Rev. B* **85**, 014,433 (2012). DOI 10.1103/PhysRevB.85.014433. URL <http://link.aps.org/doi/10.1103/PhysRevB.85.014433>
18. Gleich, B., Weizenecker, R.: Tomographic imaging using the nonlinear response of magnetic particles. *Nature* **435**(7046), 1214–1217 (2005). DOI 10.1038/nature03808
19. Gustafsson, K.: Control of error and convergence in ode solvers. Ph.D. thesis, University of Lund (1992)
20. Johannsen, M., Gneveckow, U., Thiesen, B., Taymoorian, K., Cho, C., Waldöfner, N., Scholz, R., Jordan, A., Loening, S., Wust, P.: Thermotherapy of prostate cancer using magnetic nanoparticles: feasibility, imaging, and three-dimensional temperature distribution. *European urology* **52**(6), 1653–1662 (2007)
21. Kircher, M., Mahmood, U., King, R., Weissleder, R., Josephson, L.: A multimodal nanoparticle for preoperative magnetic resonance imaging and intraoperative optical brain tumor delineation. *Cancer research* **63**(23), 8122–8125 (2003)
22. Landau, L., Lifshitz, E.: Theory of the dispersion of magnetic permeability in ferromagnetic bodies. *Phys. Z. Sowietunion* **8**, 153 (1935)
23. Lee, A., Liu, Z., Bertotti, G., Serpico, C., Mayergoyz, I.: Analysis of random magnetization switching using monte carlo simulations. *Physica B: Condensed Matter* **435**(0), 100 – 104 (2014). DOI <http://dx.doi.org/10.1016/j.physb.2013.07.020>. URL <http://www.sciencedirect.com/science/article/pii/S0921452613004420>. 9th International Symposium on Hysteresis Modeling and Micromagnetics (HMM 2013)
24. Lim, C.T., Han, J., Guck, J., Espinosa, H.: Micro and nanotechnology for biological and biomedical applications. *Medical & biological engineering & computing* **48**(10), 941–943 (2010)
25. Llandro, J., Palfreyman, J., Ionescu, A., Barnes, C.: Magnetic biosensor technologies for medical applications: a review. *Medical & Biological Engineering & Computing* **48**(10), 977–998 (2010). DOI 10.1007/s11517-010-0649-3. URL <http://dx.doi.org/10.1007/s11517-010-0649-3>
26. Néel, L.: Théorie du trainage magnétique des ferromagnétiques en grains fins avec applications aux terres cuites. *Ann. géophys* **5**(2), 99–136 (1949)
27. Nowak, U., Mryasov, O.N., Wieser, R., Guslienko, K., Chantrell, R.W.: Spin dynamics of magnetic nanoparticles: Beyond brown's theory. *Phys. Rev. B* **72**, 172,410 (2005). DOI 10.1103/PhysRevB.72.172410. URL <http://link.aps.org/doi/10.1103/PhysRevB.72.172410>
28. Pankhurst, Q., Thanh, N., Jones, S., Dobson, J.: Progress in applications of magnetic nanoparticles in biomedicine. *Journal of Physics D: Applied Physics* **42**(22), 224,001 (2009)
29. Pankhurst, Q.A., Connolly, J., Jones, S., Dobson, J.: Applications of magnetic nanoparticles in biomedicine. *Journal of physics D: Applied physics* **36**(13), R167 (2003)
30. Tan, X., Baras, J.S., Krishnaprasad, P.S.: Fast evaluation of demagnetizing field in three-dimensional micromagnetics using multipole approximation. In: *SPIE's 7th Annual International Symposium on Smart Structures and Materials*, pp. 195–201. International Society for Optics and Photonics (2000)
31. Taniguchi, T., Imamura, H.: Thermal switching rate of a ferromagnetic material with uniaxial anisotropy. *Phys. Rev. B* **85**, 184,403 (2012). DOI 10.1103/PhysRevB.85.184403. URL <http://link.aps.org/doi/10.1103/PhysRevB.85.184403>
32. Vansteenkiste, A., Van de Wiele, B.: Mumax: A new high-performance micromagnetic simulation tool. *J. Magn. Magn. Mat.* **323**(21), 2585–2591 (2011). DOI 10.1016/j.jmmm.2011.05.037. URL <https://code.google.com/p/mx3/>
33. Wiekhorst, F., Steinhoff, U., Eberbeck, D., Trahms, L.: Magnetorelaxometry assisting biomedical applications of magnetic nanoparticles. *Pharmaceutical Research* **29**, 1189–1202 (2012)